**11th International Symposium on Magnetic Bearings**
**August 26-29, Nara, Japan**

# FLEXIBLE ROTOR MODELING FOR A LARGE CAPACITY FLYWHEEL ENERGY STORAGE SYSTEM

**Seong-yeol Yoo**
Dept. of Mechatronics Eng. Chungnam National University Daejeon Korea
usyeol@cnu.ac.kr

**Cheol-hoon Park, Sang-kyu Choi**
Mechatronics Application Team Korea Institute of Machinery and Matrials
parkch@kimm.re.kr, skchoi@kimm.re.kr

**Myounggyu Noh**
Dept. of Mechatronics Eng. Chungnam National University Daejeon Korea
mnoh@cnu.ac.kr

## ABSTRACT

When we design a controller for the active magnetic bearings that support a large rotor, it is important to have an accurate model of the rotor. For the case of the flywheel that is used to store energy, an accurate rotor model is especially important because the dynamics change with respect to the running speed due to gyroscopic effects. In this paper, we present a procedure of obtaining an accurate rotor model of a large flywheel energy storage system using finite-element method. The system is designed to store 5kWh at maximum speed of 18,000 rpm. The model can predict the first and the second bending mode which match well with the experimental results obtained from a prototype flywheel energy storage system.

## INTRODUCTION

Flywheel energy storage systems (FESS) store the electric energy in terms of kinetic energy and convert this kinetic energy into electric energy when necessary. Recently, the FESS's are being actively developed for load leveling, power quality improvements and uninterruptible power supplies (UPS) because they are environmentally friendly and can sustain infinite charge/discharge cycles [1]. These systems commonly employ either passive or active non-contacting magnetic bearings to support the rotor running at high rotational speeds [2]. Typically large systems prefer active magnetic bearings (AMB) due to better damping characteristics, albeit the need of a feedback controller.

To maximize the energy storage capacity, a FESS usually choose a radially thick rotor so that the principal mass moment of inertia is larger than the transversal counterpart ($J_p / J_t > 1$). In that case, the dynamics of rotor changes significantly with respect to the running speed because of the gyroscopic effect. The flywheels may run up to near the first critical speed in order to store as much energy as possible. Thus, the controller design for the magnetic bearings must take into account the flexibility of the rotor [3]. In order to design the controller properly, therefore, it is important to have a tractable yet accurate model of the flexible rotor.

Considerable research has been done on the modeling of flexible rotor. Many authors including Jayanth *et. al.* [4], Ren *et. al.* [5], Murata *et. al.* [6], and Arredondo *et. al.* [7] studied the dynamic modeling of the small size flexible rotor. Murphy *et. al.* [8, 9] investigated the rotordynamics of a large flywheel supported by ball bearings. Hawkins and Murphy [10] described a rotordynamic model of a titanium flywheel supported by magnetic bearings.

In this paper, we present a procedure of obtaining a flexible rotordynamic model of a large composite flywheel supported by a pair of radial active magnetic bearings and a hybrid thrust bearing. The rotor model is derived by using the finite element method (FEM) [11]. The flexible rotor model thus obtained was validated against the rotor transfer function measured through experiments.

## SYSTEM DESCRIPTION

The schematic view of the system is illustrated in Figure 1. At the center of the system is a large flywheel made of double-layer fiber-reinforced composites. The flywheel is radially supported by the upper and lower active magnetic bearings. Since the magnetic bearings are open-loop unstable, the positions of the rotor are measured by a set of sensors located at the bottom and the top of the rotor, and delivered to the controller. The thrust bearing is a hybrid type where the weight of the rotor is supported by a set of permanent magnets while an electromagnetic actuator generates the dynamic control forces. The axial motion of the rotor is also measured by a position sensor. A high-speed motor/generator completes the system.

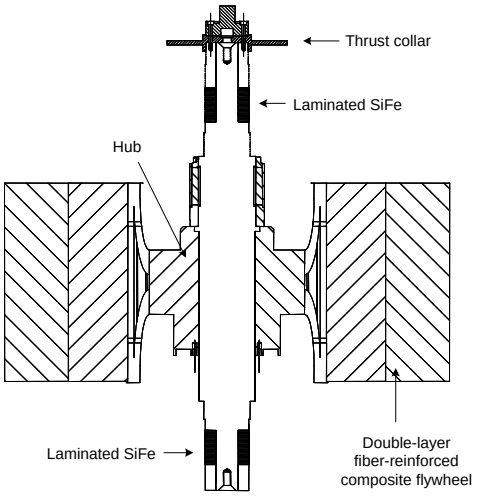


FIGURE 1. Schematic view of the rotor for a flywheel energy storage system

The flywheel system is designed to store 5 kWh as the usable energy with the maximum running speed of 18,000rpm. The rotor mass including the flywheel is 235 kg. Diameter of the flywheel is 716mm, and the axial length of the rotor is 778 mm including the thrust collar and the cap. The principal and the transverse mass moment of inertia are 13.2 kg-m$^2$ and 9.4 kg-m$^2$ respectively. The flywheel is operated in a vacuum chamber to minimize the windage loss.

The radial magnetic bearings are an eight-pole design. Two adjacent poles are wired in series and two opposing pairs control each axis of the bearing. We employed the bias linearization method for the control of the radial bearings [12], where the current in each pair of coils is the sum of the constant bias current and the control current. The current design of the bearings has the pole face area of 8.8 cm$^2$, which results in the static load capacity of approximately 1000 N per bearing, assuming the saturation density of 1.2 T. Since there are two bearings in the system, the total static load capacity in the radial direction is about 2000 N.

In order to decrease the power consumption of the thrust actuator, an opposing pair of permanent magnets is used to carry the weight of the rotor. The design of the thrust bearing depends on the force and axial stiffness of this magnet pair, which can be calculated by the equivalent current sheet method [13]. The magnets are sized so that the repulsive force is exactly the same as the weight of the rotor. The total axial force is the sum of the force by the actuator, the force by the permanent magnets and the weight of the rotor. Assuming that the maximum static loading on the thrust actuator is 1G, we can determine the size of the actuator. For the rotor which has the mass of 250 kg, the minimum pole face area is calculated to be 21.16 cm$^2$. Based on this number, we designed the thrust actuator.

For many magnetic bearing systems, decentralized control is used. In that case, each AMB is independently controlled and there is no cross coupling between the x- and y-direction. However, in the case of the system with strong gyroscopic effect, the plant dynamics changes with the rotational speed so that gyroscopic effect has to be considered for controller design. Gyroscopic effect can be compensated by cross feedback control [14]. We employed a cross feedback control with decentralized proportional-derivative (PD) controllers to compensate gyroscopic effect. The controller is implemented using xPC toolbox and Real Time Workshop [15] at the sampling rate of 10 kHz.

## SYSTEM MODELING

### Flexible rotor model

The use of finite element method (FEM) to obtain a flexible rotor model is well established. If we assume that the radial dynamics of the rotor is decoupled from the axial dynamics, we can use Rayleigh's beam theory or Timoshenko's beam theory to greatly simplify the finite element model of the rotor. In this paper, we take the approach by Nelson [16] which is succinctly described in [11]. For the sake of presentation, we will summarize the rotor model in this paper.

If we divide the rotor into many sections each of which has uniform geometry and material properties, each section (element) can be illustrated as shown in Figure 2, where $l$ is the length of the element. The origin of the local coordinates $O-xyz$ is taken at the left end of the element.

The time dependent displacement vector of the nodal point is denoted by $[u, v, \phi_x, \phi_y]^T$. The displacement vectors at the left and right ends of an element are defined as $[q_1, q_2, q_3, q_4]^T$ and $[q_5, q_6, q_7, q_8]^T$. The infinitesimal thickness of a sliced disk at the position $s$ is $ds$. Since the rotations $\phi_x$, $\phi_y$ have the differential relationships with the translations $u, v$ with respect to $ds$, the quantities $u, v$ can be defined by linear combinations with shape functions. The resulting equations of motion for the element are described as

$$\mathbf{m_e}\ddot{\mathbf{q}} + \mathbf{g_e}\dot{\mathbf{q}} + \mathbf{k_e}\mathbf{q} = \mathbf{f_e} \tag{1}$$

The vectors $\mathbf{q}, \mathbf{f_e}$ are the displacements and the forces respectively. The matrices $\mathbf{m_e}$, $\mathbf{g_e}$, $\mathbf{k_e}$ are the mass matrix, gyroscopic matrix, and stiffness matrix of the element respectively. In order to obtain equation of motion for entire rotor, we have to apply boundary conditions between each element. Then governing equation of complete rotor can be written as

$$\mathbf{M}\ddot{\mathbf{Q}} + \mathbf{G}\dot{\mathbf{Q}} + \mathbf{K}\mathbf{Q} = \mathbf{F} \tag{2}$$

where the global mass, gyroscopic, and stiffness matrices are assembled from the element matrices as

$$\mathbf{M} = \sum_{i=1}^{n} \mathbf{m}_e^i, \quad \mathbf{G} = \sum_{i=1}^{n} \mathbf{g}_e^i, \quad \mathbf{K} = \sum_{i=1}^{n} \mathbf{k}_e^i \tag{3}$$

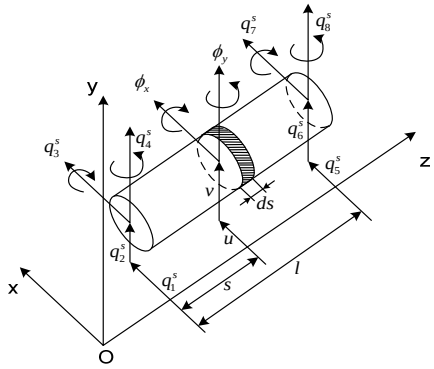


FIGURE 2. Typical rotor element and coordinates [11].

### Active Magnetic Bearing Model

If the bias linearization method is used for the control of active magnetic bearings, we can obtain a linear model of the bearing, assuming that the rotor displacements are small. Using the notations used in (2), we can express this linear model as

$$\mathbf{F} = -\mathbf{K}_x\mathbf{Q} + \mathbf{K}_a\mathbf{u} \tag{4}$$

where the bearing stiffness matrix $\mathbf{K}_x$ and the actuator gain matrix $\mathbf{K}_a$ are calculated from the parameters of the bearing such as the nominal air gap, the number of turns per pole, and the pole area. Combining (2) and (4), and defining a state vector as

$$\mathbf{x} = \begin{bmatrix} \mathbf{Q} \\ \dot{\mathbf{Q}} \end{bmatrix} \tag{5}$$

we can obtain a model for the rotor suspended by a set of active magnetic bearings as follows.

$$\dot{\mathbf{x}} = \begin{bmatrix} \mathbf{0} & \mathbf{I} \\ -\mathbf{M}^{-1}(\mathbf{K}+\mathbf{K}_x) & -\mathbf{M}^{-1}\mathbf{G} \end{bmatrix}\mathbf{x} + \begin{bmatrix} \mathbf{0} \\ \mathbf{M}^{-1}\mathbf{K}_a \end{bmatrix}\mathbf{u} \tag{6}$$

### Sensor and Controller Model

As mentioned previously, a set of position sensors measure the position of the rotor and provide feedback signal for the controller. The simple model of the rotor would be just selecting appropriate nodal coordinates where the sensors are locating. Typically, the sensor signals are put to pass through a filter. Then the sensor model can be conveniently expressed in a transfer function format as

$$y = H(s)x \tag{7}$$

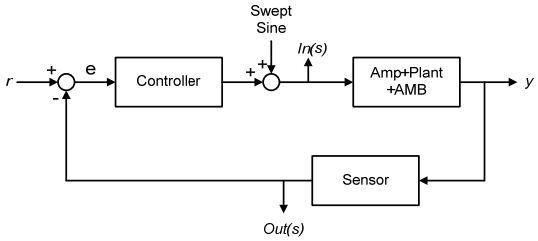


FIGURE 3. Block diagram for FRF

Also, the PD controller with a cross feedback can be expressed in terms of a transfer function as

$$u = C(s)y \tag{8}$$

The system model can be obtained by combining (6), (7), and (8). Because the gyroscopic matrix **G** in (6) is dependent on the speed, the dynamics of the whole system is speed-dependent.

## EXPERIMENTS AND SIMULATION RESULTS

We obtained the experimental rotor transfer function from the system for the purpose of validating the flexible rotor model we derived. We injected test signals into the controller output and then measured the rotor response signals from the sensors (shown in Figure 3). Using swept sine signal as a test signal [17], we can calculate the frequency response function (FRF) from

$$FRF(s) = \frac{Out(s)}{In(s)} \tag{9}$$

The dotted lines in Fig. 4 are the frequency response functions measured from the upper and lower position sensors. These frequency response functions represent the dynamics of the plant which includes the rotor, active

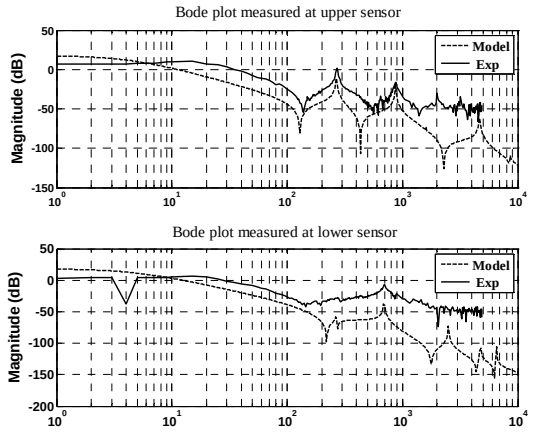


FIGURE 4. Comparison of bode plots of FRF and model simulation for upper and lower AMB

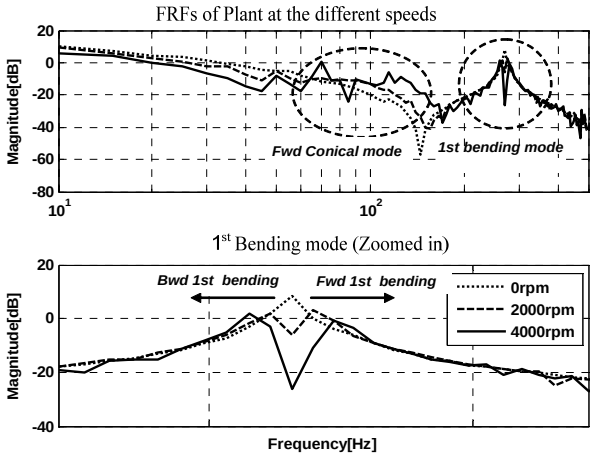


FIGURE 5. Comparisons of FRFs of Upper AMB at the different speeds

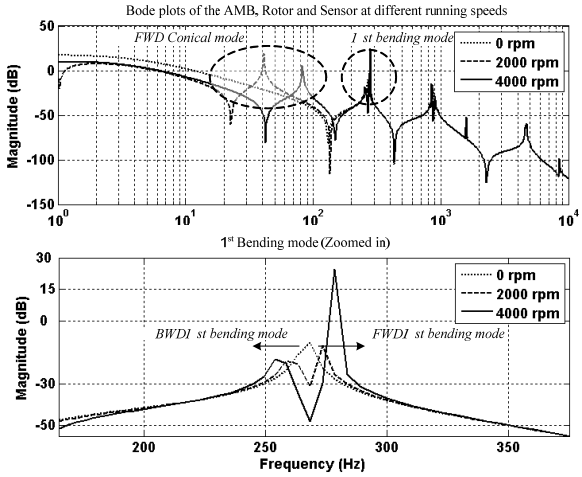


FIGURE 6. Comparison of bode plots of upper AMB at the different speed (simulation)

magnetic bearings, amplifiers and sensors while the rotor is at standstill. The upper FRF shows the first bending mode at 270 Hz and the second bending mode at 880Hz. The lower section of the rotor has somewhat higher first bending mode at 700Hz. The solid lines in Fig. 4 are the frequency response functions calculated from the flexible rotor model we derived earlier. The model predicts the first and second bending modes fairly accurately. Since the sampling rate is 10 kHz, we expect somewhat distorted FRFs close to 5 kHz.

Experimental results confirm the strong gyroscopic coupling of the flywheel. Figure 5 shows the frequency response functions at several different running speeds. The forward conical mode appears before 4000 rpm and the first bending mode splits with the increasing running speed. Simulation model also exhibits the similar behavior with respect to the running speed, which is shown in Figure 6. Simulated results show that the forward conical mode appears before 2000 rpm which is lower than the experimental result. The discrepancy may be due to the modeling of the discrete disks and flywheel which we consider as concentrated mass.

Figure 7 shows the Campbell diagram that summarizes the dynamics of the rotor. In Fig. 7, the first bending mode splits into forward and backward mode as previously noted in Fig. 5 and 6, and the behavior of the forward conical mode matches well with the simulation results.

We ran the flywheel up to 9,000 rpm, and measure the sensitivity at several different running speeds. As shown in Fig. 8, the sensitivity has a peak at around 120 Hz when the running speed is 3,000 rpm. This peak is the source of poor stability [18] and is caused by the forward conical mode, which is another evidence of the strong gyroscopic coupling. To run through this mode, we added notch filters to the decentralized PD controllers of both magnetic bearings. Figure 9 is a waterfall plot measured from the upper sensor from 0 rpm to 9,000 rpm. The waterfall plot indicates that the the synchronous vibration is the major disturbance to the system.

## CONCLUSIONS

Having an accurate rotor model is very important to properly design the controller of the system especially whose dynamics changes with the running speed. However, it is usually difficult to model the flexible rotor because many flexible disks or blades are mounted on the rotor. In this paper, we used FEM to derive a flexible rotor model for 5kWh flywheel energy storage system. The rotor model predicts well the first and the second bending mode of the upper section of the rotor, and the first bending mode of its lower section. We ran a prototype 5kWh FESS up to 9,000 rpm which is well below the target speed. Decentralized PD controllers with cross feedback were not able to provide sufficient stability that is required to achieve the target speed. We are currently evaluating other forms of controller such as MIMO controller and gain scheduling [10].

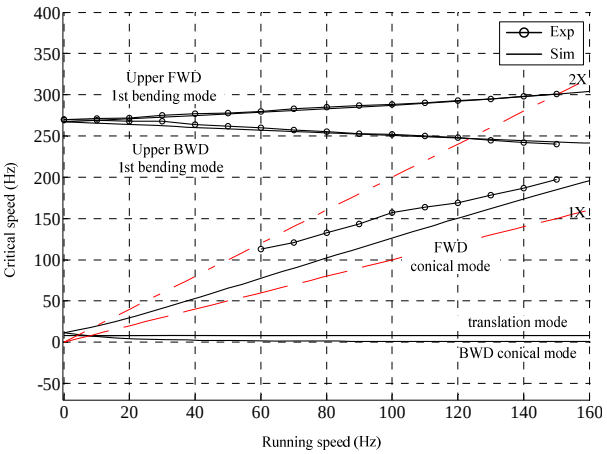


FIGURE 7. Simulated and measured Campbell diagram of the rotor.

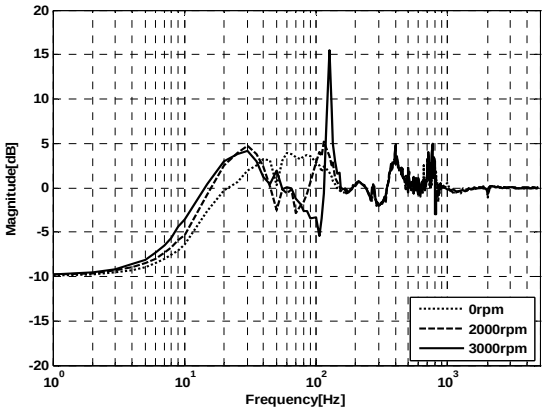


FIGURE. 8 Comparison of Sensitivity Transfer Function of FESS at the different speeds (measured from the upper sensor)

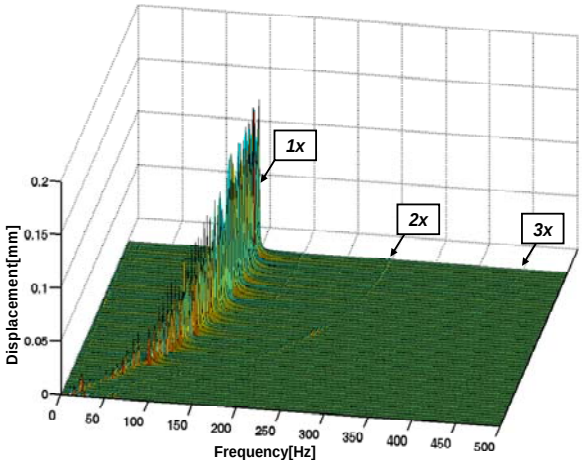


FIGURE 9 Waterfall plot measured from the upper sensor during spin up from 0 rpm to 9000 rpm

**REFERECES**


[1] N. Koshizuka, *et. al*., "Present status of R & D on superconducting magnetic bearing technologies for flywheel energy storage system," Physica C-Superconductivity and Its Applications, vol. 378, pp. 11-17, Oct 1 2002.

[2] S. Sivrioglu and K. Nonami, "Active permanent magnet support for a superconducting magnetic-bearing flywheel rotor," IEEE Transactions on Applied Superconductivity, vol. 10, pp. 1673-1677, Dec 2000.

[3] K. Nonami and T. Ito, " $\mu$ synthesis of flexible rotor-magnetic bearing systems," IEEE Transactions on Control Systems Technology, vol. 4, pp. 503-512, Sep 1996.

[4] V. Jayanth, H. Choi, and G. Buckner, Identification and Control of a Flexible Rotor Supported on Active Magnetic Bearings, Proc. of IEEE SoutheastCon, 2002.

[5] M. Ren, K. Nonami, A. Kubo, and H. Kameno, Zero Bias $H_\infty$ Control of Flexible Rotor Magnetic Bearing Flywheel System with Gyroscopic Effect Using Singular Value Decomposition, 10th Int. Symp. On Magnetic Bearings, Martigny, Switzerland, 2006.

[6] M. Murata, H. Tajima, T. Watanabe, and K. Seto, New Modeling and Control Methods for Flexible Rotors with Magnetic Bearings toward Passing through Critical Speeds caused by Elastic Modes, 10th Int. Symp. On Magnetic Bearings, Martigny, Switzeland, 2006.

[7] I. Arredondo, J. Jugo, and V. Etxebarria, Modeling and Control of a Flexible Rotor System with AMB-based Sustentation, ISA Trans. 47, pp. 101-112, 2008.

[8] B. Murphy, S. Manifold and J. Kitzmiller, Compulsator Rotordynamics and Suspension Design, IEEE Trans. on Magnetics, Vol. 33, No. 1, 1997.

[9] B. Murphy, J. Kitzmiller, R. Zowarka, J. Hahne, and A. walls, Rotordynamics Design and Test Results for a Model Scale Compulsator Rotor, IEEE Trans. on Magnetics, Vol. 37, No. 1, 2001.

[10] L. Hawkins, B. Murphy, and J. Kajs, Analysis and Testing of a Magnetic Bearing Energy Storage Flywheel with Gain-Scheduled, MIMO Control, Proc. of ASME Turboexpo2000, Munich Germany, 2000

[11] .T. Yamamoto and Y. Ishida, Linear and Nonlinear Rotordynamics: A Modern Treatment with Applications. New York: John Wiley & Sons, 2001.

[12] E. H. Maslen and D. C. Meeker, "Fault tolerance of magnetic bearings by generalized bias current linearization," IEEE Trans. Magnetics, vol. 31, pp. 2304-2314, May 1995.

[13] C. Chen *et al*., "A magnetic suspension theory and its application to the HeartQuest ventricular assist device," Artif. Organs, vol. 26, pp. 947-951, 2002.

[14] M. Ahrens, L. Kucera and R. Larsonneur, "Performance of a magnetically suspended flywheel energy storage device," IEEE Trans. Contr. Syst. Tech., vol. 4, pp. 494-502, Sept. 1996.

[15] xPC toolbox and MATLAB, The Mathworks Corporation, Cambridge, USA.

[16] H. D. Nelson, J. M. McVaugh, "The dynamics of rotor-bearing systems using finite elements," ASME Journal of Eng. For Ind., vol. 98, pp593-600, May 1976.

[17] C. H. Park, S. K. Choi, J. P. Lee and Y. H. Han, "On the Dynamic Behavior of a 5kWh FESS Mounted on AMBs," The 11th Internaltional Conference on Mechatronics Technology, pp. 416-420, 2007.

[18] G. Li, E. H. Maslen and P. E. Allaire, "A Note on ISO AMB Stability Margin,", 10th International Symposium on Magnetic Bearings, Martigny, Switzerland, 2006.